International Journal of Fracture manuscript No.
(will be inserted by the editor)

Validity of linear elasticity in the crack-tip region of ideal brittle solids

Gaurav Singh · J. R. Kermode · A. De Vita · R. W. Zimmerman

Received: date / Accepted: date

Abstract It is a well known that, according to classical elasticity, the stress in the crack-tip region is singular, which has led to a debate over the validity of linear elasticity in this region. In this work, comparisons of finite and small strain theories have been made in the crack-tip region of a brittle crystal to comment on the validity of linear elasticity in the crack tip region. We find that linear elasticity is capable of accurately defining the state of stress very close ($\sim$1 nm) to a static crack tip.

Keywords crack · singularity · elasticity · brittle

1 Introduction

Early work by Irwin (1948) shows that a crack gives rise to a stress field with a singularity at the tip. This prediction of infinite stress at the crack tip has led to much debate regarding whether linear elasticity theory is valid in the crack-tip region. The crack-tip region has often been considered specially in fracture mechanics, with non-linearity and plasticity associated with it in some form or other (Broberg 1971). For ceramics, there have been theories of a competing (quasi) plasticity with brittleness (Rhee *et al.* 2001). Experimental observations of cracks in glass have been taken as indicators of the presence of non-linearity in crack-tip regions (Xi *et al.* 2005). On the other hand, linear elasticity has been argued for brittle materials (Goldstein and Salganik 1974). From the continuum perspective, a number of suggestions have been made to remove the unrealistic infinite stresses, including the inclusion of cohesive forces (Barenblatt 1962), the introduction of plasticity (Cherepanov 1967), and the use of finite strains (Wong and Shield 1969), among other techniques. The first two of these approaches do not have an obvious correspondence with atomistic simulations, and so the third option will be investigated in the present work to test the validity of the infinitesimal strain theory in the near-tip region.

Until relatively recently, most modelling of failure in brittle materials has been carried out at the continuum level (Freund 1998; Lawn 1993), following the energy-balance analysis first presented by Griffith (1921). These techniques have been sufficient to describe brittle fracture in carefully prepared single crystal samples (Cramer *et al.* 2000). However, in more complicated situations atomistic details become increasingly relevant.

Analytically solvable lattice models (Slepyan 2002) have been used to show that the discreteness of an atomic lattice can impose constraints on accessible steady-state crack velocities at low temperatures, leading to the "velocity gap" concept (Marder and Liu 1993), and the related phenomenon of "lattice trapping" whereby cracks are inhibited until the load is increased above that predicted by the Griffith energy-balance approach (Thomson *et al.* 1971; Holland and Marder 1998). Moving from lattice models to an explicitly atomistic description of fracture has proven to be difficult. This is largely because a combination of high accuracy and large system sizes is needed to accurately model failure in materials. On one hand, the ionic or covalent bond breaking and formation associated with crack advancement requires interatomic potentials capable of quantum mechanical (QM)

Gaurav Singh, R. W. Zimmerman
Department of Earth Science & Engineering, Imperial College London, London UK SW7 2AZ
E-mail: r.w.zimmerman@imperial.ac.uk

J. R. Kermode
King's College London, Department of Physics, London UK WC2R 2LS
E-mail: james.kermode@kcl.ac.uk

A. De Vita
King's College London, Department of Physics, London UK WC2R 2LS
CENMAT-UTS, Via A. Valerio 2, 34127 Trieste, Italy

accuracy. On the other hand, the need to capture long-range stress concentrations requires large-scale ($\sim 10^6$ atoms) model systems as well as accurate molecular dynamics (MD) schemes. Despite these competing difficulties, recent advances in highly accurate MD schemes have led to both qualitative and quantitative insights into the mechanisms underlying brittle fracture of real materials (Bernstein and Hess 2003; Buehler *et al.* 2006; Kermode *et al.* 2008, 2013; Gleizer et al. 2014).

Most of the focus of atomic-scale fracture research has, however, been on modelling the physical and chemical behaviour using sophisticated methods. The definitions of strain and stress, originally purely continuum concepts, have not been the subject of such intense focus at the atomic level. Instead, stresses are typically extracted from atomistic simulations using the virial stress tensor, which is a measure of mechanical stress at the atomic scale derived from the virial theorem, and defined at zero temperature by

$$\sigma_{ij} = \frac{1}{\Omega} \sum_{p \in \Omega} \frac{1}{2} \sum_{q \in \Omega} (x_i^{(q)} - x_i^{(p)}) f_j^{(pq)} \qquad (1)$$

where p and q are atom indices, i, j, k are Cartesian indices, Ω is the cell volume, $x^{(p)}$ is the position of atom p, and $f_j^{(pq)}$ is the jth component of the force between the atoms p and q (Cramer *et al.* 2000). The force between the atoms is calculated using interatomic potentials. This expression is often used to define a local atomic stress, and hence also a local atomic virial strain (Buehler 2008); however, it has been shown that this procedure leads to unphysical oscillations, since the virial theorem only applies when averaged over time and space (Zimmerman *et al.* 2004).

Finding a link between atomic simulations and continuum mechanics is of considerable interest to both communities, and there is a large research effort aimed at constructing multi-scale simulations which directly couple atomic and finite element descriptions, for example, the Quasi-Continuum approach of Tadmor *et al.* (1996) and the QM-CADD approach of Nair *et al.* (2010). The long-wavelength limit of an atomic lattice has been shown to reproduce continuum results, demonstrating that classical elasticity remains valid at the nanoscale for a number of materials (Maranganti and Sharma 2007). However, the ability of linear elasticity to describe the very large strains and strain gradients that occur within a few nanometers of a crack tip has not yet been investigated in detail.

The focus in this work is on a specific case: mode I fracture on the (111) cleavage plane in a single crystal of silicon, which is an example of a perfectly brittle process that can be well described at the atomic scale (Kermode *et al.* 2008). The classical interatomic potential proposed by Stillinger and Weber (1985) will be employed, which has been widely used to study many properties of silicon. Comparisons of the resulting stress fields to an analytical continuum solution are also made (Knauss 1966).

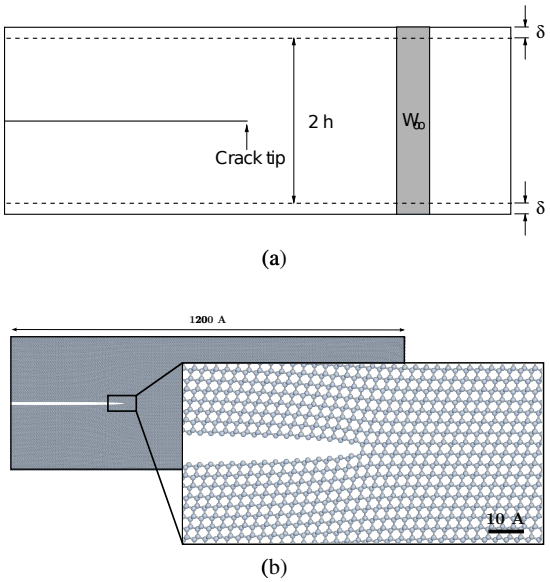

Fig. 1: (a) Thin strip loading geometry. The edges of the strip are clamped and displaced vertically by an amount δ. The energy density far ahead of the crack tip is W_∞. (b) Relaxed atomic coordinates of 90,000 atom silicon $(111)[1\bar{1}0]$ crack system under applied load of $G = 1.75$ J/m^2 (below $G_c = 2\gamma_{111} = 2.72$ J/m^2); inset shows close up of crack tip, with a horizontal field of view of 100 Å.

2 Description of Molecular Statics Simulation

The objective of the present work is to check if linear elasticity is sufficient to accurately describe the stress in the crack-tip region. Therefore, the energy release rate of $G = 0.64G_c = 1.75$ J/m^2 has been chosen to be below the Griffith threshold but still high enough not to close up at zero temperature (i.e., it is within the range of "lattice trapped" loads (Thomson *et al.* 1971; Bernstein and Hess 2003)).

For the widely-used thin strip geometry shown in Figure 1, the strain energy release rate (SERR) is independent of crack length and can be calculated analytically following the approach of Rivlin (1953), and subsequently used by Holland and Marder (1998); Swadener *et al.* (2002). Periodic boundary conditions are used in the out-of-plane direction, corresponding to plane strain conditions. It has been shown that the correct limiting behaviour can be reached, for a dynamical simulation with increasing load, with reasonably modest system sizes containing thousands or tens of thousands of atoms (Marder 2004). Even though no dynamic simulations are required in the present work, these previous works ensure that the system is sufficiently large to accomodate the required strain gradients.

The thin strip setup was utilised to apply load to a single crystal silicon model with dimensions 120 nm $\times$ 40 nm $\times$ 0.384 nm, containing 90,000 atoms, and oriented to expose

a (111) cleavage plane and a $[1\bar{1}0]$ crack front (Fig. 1b). The equilibrium atomic positions, in the unstressed and stressed states, were calculated using the Stillinger-Weber (SW) potential, as implemented in the QUIP molecular dynamics package (Csányi *et al.* 2007). The classical interatomic potential proposed by Stillinger and Weber (1985) has been widely used to study many properties of silicon. Whilst this potential does not correctly describe the dynamics of fracture (Holland and Marder 1998), it has been shown to provide a good description of the stress concentration phenomena (Kermode *et al.* 2008). Since the objective of this present work is limited to study of the stress state in the crack-tip region, the use of this potential is acceptable.

The deformed coordinates of the atoms (after relaxation) were then extracted to find the strains, as explained in Section 3. It is worth mentioning that even though atomistic simulation is intrinsically three-dimensional, to carry out the strain calculations, the system of atoms was projected onto a two-dimensional plane (consistent with the plane strain boundary conditions).

3 Calculation of Finite Strain

In this section, the continuum theory of finite deformation (Mal and Singh 1991) will be applied to the atomic scale, along with the methodology for the calculation of strain.

3.1 Deformation Gradient and Strain

A solid body is distributed over a region of space. Every geometrical point in this continuum solid is occupied by a small element of solid at all times. This differential solid element will be referred to as a "point" from here on.

It is known that application of a load will deform the body. This implies that some of these points will be displaced from their original positions. To differentiate between the original and the deformed configurations of the points before (0) and after (t) the application of the load, the symbols R_0 and R_t will be used to denote the mathematical space occupied by the points. The points in these configurations are denoted by their coordinates X_I $(I = 1,2)$ $[\mathbf{X} \in R_0]$ and x_i $(i = 1,2)$ $[\mathbf{x} \in R_t]$, respectively. For simplicity, both R_0 and R_t will be assumed to have the same Cartesian vector basis. The motion of the concerned point P is described by the mapping

$$\mathbf{x} = \chi(\mathbf{X}) \tag{2}$$

where χ is assumed to be continuously differentiable with respect to $\mathbf{X}$. If the point P occupying the position X_I in the original space R_0 has *quasi-statically* moved to occupy the position x_i in the deformed space R_t where Equation 2 holds, another neighbouring point P' originally located at $X_I + \Delta X_I$ in R_0 will have therefore moved to $x_i + \Delta x_i$ in R_t. The deformation gradient tensor can now be defined as

$$F_{iI} = \lim_{\Delta X_I \to 0} \frac{\chi(X_I + \Delta X_I) - \chi(X_I)}{X_I + \Delta X_I - X_I} = \frac{\partial x_i}{\partial X_I} \tag{3}$$

The deformation gradient F_{iI} gives a complete description of the deformation of the solid in the immediate neighbourhood of the point P (Mal and Singh 1991). The finite strain tensor is defined as

$$\mathbf{E} = \frac{1}{2}(\mathbf{F}^T\mathbf{F} - \mathbf{I}) \tag{4}$$

whereas the infinitesimal strain tensor is defined as

$$\mathbf{e} = \frac{1}{2}((\mathbf{F} - \mathbf{I}) + (\mathbf{F} - \mathbf{I})^T) \tag{5}$$

where the superscript T denotes the transpose of a matrix, and $\mathbf{I}$ is the identity matrix of a suitable order. The finite strain tensor and the infinitesimal strain tensor are close to each other, according to some appropriate metric, when the strains are "small".

After having gone through the above discussion for a continuum solid, it can be argued that the definitions of deformation gradient and strain must hold for a discrete atomic system, if the points P and P' of the continuum are identified with the centre-point of the atom ("atom" from here on). Thus, the displacement of the continuum points would correspond to the displacement of the atoms.

3.2 Homogeneous Deformation

The definition of the deformation gradient, which is needed to calculate the strain, requires a differentiation operation to be conducted. To allow this, the position of the atoms will first be fit with linear and quadratic functions, which can then be analytically differentiated. These functions must be applied in a *local* region around the reference atom to justify the condition of $\Delta X_I \to 0$ used in the definition of the deformation gradient.

For a linear transformation (Love 1920), the deformed position of the atom can be expressed in the form

$$x_i = a_{ij}X_j + b_i \tag{6}$$

where a_{ij} and b_i are constants that are independent of X_j, and $i, j = 1,2$ for a two-dimensional system. To find the fitting parameters a_{ij} and b_i in the above expression, the sum of the squares of the error between the observed and the expected values of the deformed location of each atom must be minimized. Although inclusion of displacement information from additional neighbouring atoms will, in principle, result in more accurate curve fits, it will, however, make the system less *local*. For the linear fit, using four neighbouring atoms has been found to be sufficient for giving accurate results. Thereafter, the deformation gradient F_{iI} and the strain $\mathbf{E}$ can be easily computed.

In the present work, the above technique has been extended for the quadratic deformation function, in which the deformed position of the atom can be expressed in the form

$$x_i = a_{ijk}X_jX_k + b_{ij}X_j + c_i \tag{7}$$

where a_{ijk}, b_{ij} and c_i are constants independent of X_j, and $i,j,k = 1,2$. This is done to see if this gives more accurate results compared to the linear approximation. It is worth mentioning that the non-linearity in the description of positional change is fundamentally independent with the non-linearity in elasticity as a general case; the latter has been discussed extensively in the literature (Geubelle and Knauss 1994). The parameters a_{ijk}, b_{ij} and c_i are found using the same technique as that of linear deformation function. As the number of unknowns in the quadratic deformation fit is greater than in the linear fit, the displacement information from a greater number of atoms is needed. The minimum number of such atoms turns out to be ten (the reference atom being one of them).

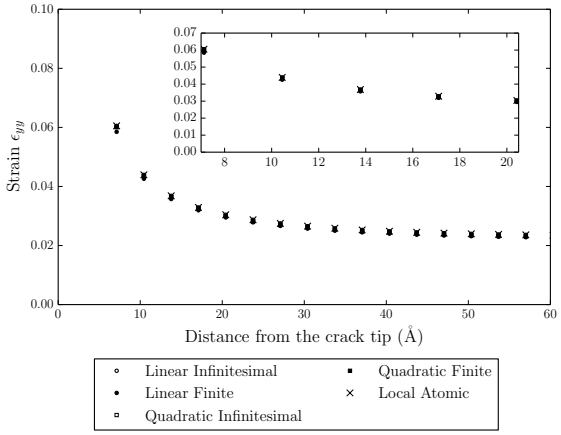

Fig. 2: Strain components ε_{yy} along the line ahead of the crack tip, computed using a variety of methods. Points correspond to atom sites, and inset shows near-tip region.

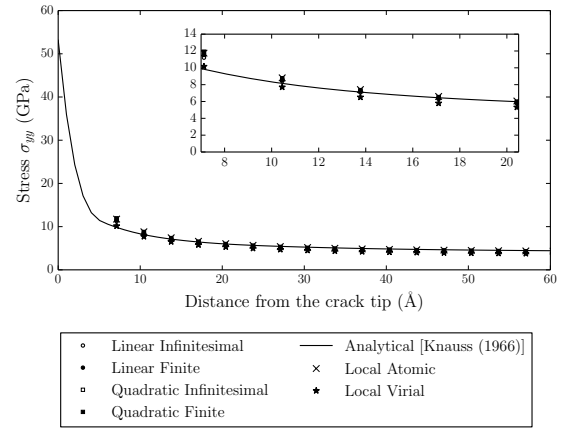

Fig. 3: Stress component σ_{yy} along the line ahead of the crack tip, computed using a variety of methods. Points correspond to atom sites, and inset shows near-tip region.

4 Results

4.1 Strain

The strain ε_{yy} along the line ahead of the crack tip for the system of Figure 1 has been calculated, using a variety of methods: the linear and quadratic deformation approximations, according to both the finite and infinitesimal strain definitions. The results are shown in Figure 2 from the third atom from the crack tip. For the first two atoms, there are not enough uniformly-spread neighbouring atoms in the bulk to accurately use linear and quadratic homogeneous deformation functions. Also shown in the figure is the strain calculated using the atom-resolved strain tensor (Moras *et al.* 2010), which essentially amounts to computing the symmetric contribution to the local deformation associated with displacement of the four neighbours of each Si atom from the positions they would adopt in a perfect crystal.

There is only a minor (essentially negligible) difference between the infinitesimal and finite strains calculated for both the linear and the quadratic descriptions of the deformation. This gives indications that infinitesimal strain theory is valid in the near-tip region. Moreover, the agreement with the local atomic strain is also very good.

4.2 Stress

The stress tensor σ_{ij} is next computed at an atomic level within the theory of linear elasticity using Hooke's law $\sigma = \mathbf{C}\varepsilon$, where $\mathbf{C}$ is the elasticity tensor (the values of which are derived using the SW interatomic potential and crystal structure) specified in the Appendix, and σ and ε are the stress and strain tensors. (We will see later that using linear elasticity here is sufficient).

From the plots for stress σ_{yy} in Figure 3, similar observations to those of strain can be made. Specifically, there is generally good agreement between all the methods, indicating that infinitesimal strain and locally linear deformation approximation are sufficient assumptions. In addition to the stresses calculated from the strains of Subsection 4.1, Figure 3 also shows the analytical continuum solution to the problem discussed originally derived by Knauss (1966). The worst mismatch occurs at the third atom from the crack tip, but this stress is still within 20% of the analytical approximation. The local atomic stress results (plotted with crosses) were calculated by applying Hooke's law to the lo-

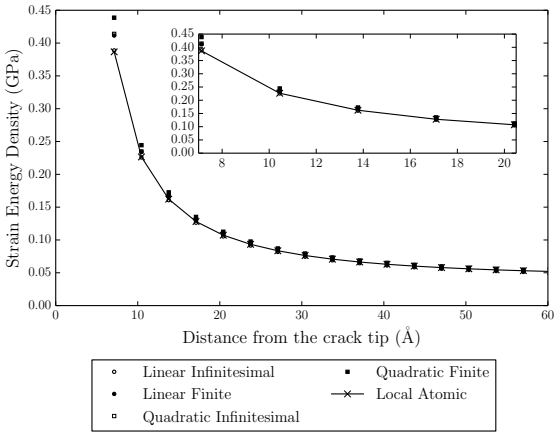

Fig. 4: Strain energy density along the line ahead of a crack tip, computed using a variety of methods. Points correspond to atom sites, and inset shows the near-tip region.

cal atomic strain described above, and again the agreement with the other methods is good. Finally, stresses computed using the virial tensor of Eq. 1 are shown with stars. Here, the agreement is much less good, consistent with the conclusions of Zimmerman *et al.* (2004), and lending support to our focus on local strain, however computed, as the best way to combine continuum and atomistic results.

The analytical results were derived for an isotropic medium, whereas the crystalline silicon is anisotropic. For the present comparison, the stresses were calculated from the analytical solution by using the Young's modulus in the relevant crystallographic direction (Kermode *et al.* 2008). Very recently the analytical solution has been extended to the fully anisotropic case by Chaudhuri (2014); comparions with this approach are planned for future work.

The strain energy density at each atomic site i can be evaluated straightforwardly as $U^i = \frac{1}{2}\sigma^i_{mn}\varepsilon^i_{mn}$ where σ^i_{mn} and ε^i_{mn} are the stress and the strain tensors, respectively, at the atomic site i. While the good agreement between the strain energy densities computed with the various methods outlined above seen in Figure 4 follows trivially from the results for stress and strain, we also observe good agreement between the Hooke's law strain energy density and the values calculated directly using the Stillinger-Weber interatomic potential. The closest match to the potential energy is found when the energy density is computed using infinitesimal strain and the linear deformation function. This justifies the use of linear elasticity for calculating the stresses above.

5 Conclusion

Our results show that stresses computed from atomistic simulations of the deformation around a static crack tip in silicon agree closely with those computed from the analytical solution of the continuum equations, for distances as low as $\sim$1 nm (about three atoms) from the crack tip. Long-standing concerns that the singular stresses predicted by the analytical solution would render the solution invalid seem to be unwarranted, at least for the static situation considered here. (We note that the failure of this method for the first two atoms from the crack-tip does not imply a failure of the linear elastic model: for the first two atoms, there are not enough uniformly-spread neighbouring atoms in a bulk coordination arrangement to accurately use linear and quadratic homogeneous deformation functions).

These results should be contrasted with, for example, the work of Barenblatt (1962) which suggests that it is necessary to invoke cohesive forces to cancel out the analytical singularity, or arguments that appeal to a small region of plastic deformation in the crack-tip region. Our results suggest that the stresses in this region remain large but finite very close to the crack tip, and can be modelled using linear elasticity. Similar large and non-singular stresses have been observed in crystals in realistic environmental conditions (Gerberich *et al.* 1991). We note that two points of view have typically been adopted when modelling stress fields very close to a crack tip. Non-linearity was generally acknowledged in both viewpoints, and either ignored since the tip is small, for example Goldstein and Salganik (1974), or corrected for using plasticity or other dissipation models, for example Xi *et al.* (2005). Direct comparions of the kind we suggest here provide one way to help reconcile this discrepancy.

Our results suggest that it is possible to apply linear elasticity very close to a crack tip during quasi-static failure of an ideally brittle material containing no other defects. Predicting the dynamic fracture response is inherently more complex than the static case studied here, and for many materials can only be modelled correctly using hybrid QM/MM (quantum mechanical/molecular mechanical), due to the combination of size and accuracy requirements. While such ideal materials are rare in realistic situations, close-to-perfect single crystals of silicon are available and can provide model materials in which simulations and experiments can be quantitatively compared (Kermode *et al.* 2013; Gleizer et al. 2014). The results presented here provide useful information to help carry out accurate studies of dynamic fracture using hybrid techniques, which, due to the very high $O(N^3_{\mathrm{atoms}})$ cost of standard QM techniques, benefit hugely from being able to assume a nanoscale QM process zone. The validity of infinitesimal strain theory in other perfectly brittle materials such as, e.g., diamond, sapphire and glass could be tested in future following the approach presented here. In the longer term, the results of such calculations could be used to bring continuum models down to scales at which atomistic input is available, which could be useful, e.g., for the calibration of improved damage models.

Appendix

The elasticity tensor c_{ijkl} linearly relates the stress tensor σ_{ij} to the strain tensor ε_{ij} as $\sigma_{ij} = c_{ijkl}\varepsilon_{ij}$. Symmetries of $\mathbf{c}$ and ε, and the requirement for the strain energy to be positive definite, reduce the fourth order tensor c_{ijkl} to a 6×6 matrix C_{ij}. For cubic cystal symmetry C_{ij} has three independent elements and takes the form

$$\begin{pmatrix} C_{11} & C_{12} & C_{12} & 0 & 0 & 0 \\ C_{12} & C_{11} & C_{12} & 0 & 0 & 0 \\ C_{12} & C_{12} & C_{11} & 0 & 0 & 0 \\ 0 & 0 & 0 & C_{44} & 0 & 0 \\ 0 & 0 & 0 & 0 & C_{44} & 0 \\ 0 & 0 & 0 & 0 & 0 & C_{44} \end{pmatrix}$$

where $C_{11} = 151.35$ GPa, $C_{12} = 76.409$ GPa and $C_{44} = 56.422$ GPa in the atomic crystal frame of reference (Kermode *et al.* 2008). This elasticity tensor has to be rotated from the crystal frame to the sample frame ($x = [11\bar{2}]$, $y = [111]$, $z = [1\bar{1}0]$), corresponding to cleavage along the lowest energy (111) cleavage plane.

Acknowledgements We acknowledge funding from the Rio Tinto Centre for Advanced Mineral Recovery based at Imperial College, London, and useful discussions with Gert van Hout throughout the project. J.R.K and A.D.V. acknowledge funding from the EPSRC HEmS Grant EP/L014742/1 and from the European Commission ADGLASS FP7 project.

References

Barenblatt GI (1962) The mathematical theory of equilibrium cracks in brittle fracture. Adv. Appl. Mech., 7:55-129

Bernstein N, Hess DW (2003) Lattice Trapping Barriers to Brittle Fracture. Phys. Rev. Lett., 91:25501-4

Broberg KB (1971) Crack-growth criteria and non-linear fracture mechanics. J. Mech. Phys. Solids. 19(6):407-418

Buehler M, van Duin A, Goddard W Phys. Rev. Lett. 96:95505

Buehler, M (2008) Atomistic Modeling of Materials Failure. Springer, Boston

Camacho GT, Ortiz M (1996) Computational modelling of impact damage in brittle materials. Int. J. Solids Struct. 33(20-22): 2899-2938

Chaudhuri RA (2014) Int. J. Fract., in press, DOI 10.1007/s10704-013-9891-7

Cherepanov GP (1967) Crack propagation in continuous media. J. Appl. Math. Mech., 31(3):503-512

Cramer T, Wanner A, Gumbsch P (2000) Energy dissipation and path instabilities in dynamic fracture of silicon single crystals. Phys. Rev. Lett., 85(4):788-791

Csányi G, Winfield S, Kermode JR, De Vita A, Comisso A, Bernstein N, Payne MC. Expressive Programming for Computational Physics in Fortran 95+. IoP Computational Physics Newsletter, Code available from `http://www.libatoms.org`.

Freund LB (1998) Dynamic fracture mechanics. Cambridge University Press, Cambridge.

Gerberich WW, Oriani RA, Lji MJ, Chen X, Foecke T (1991) The necessity of both plasticity and brittleness in the fracture thresholds of iron. Philos. Mag. A. 63(2): 363-376

Geubelle PH, Knauss WG (1994) Finite strains at the tip of a crack in a sheet of hyperelastic material: I. Homogeneous case. J. Elast., 35:61-98

Gleizer A, Peralta G, Kermode JR, De Vita A, and Sherman D (2014), Phys. Rev. Lett. 112, 115501.

Gol'dstein RV, Salganik RL (1974) Brittle fracture of solids with arbitrary cracks. Int. J. Fract. 10(4): 507-523

Griffith AA (1921) The phenomena of rupture and flow in solids. Philos. Trans. R. Soc. London, Ser. A, 221:163-198

Holland D, Marder M (1998) Ideal brittle fracture of silicon studied with molecular dynamics. Phys. Rev. Lett., 80(4):746-749

Irwin GR (1948) Fracturing of metals. Trans. Am. Soc. Met., 40:147

Kermode JR, Albaret T, Sherman D, Bernstein N, Gumbsch P, Payne MC, Csanyi G, De Vita A (2008) Low-speed fracture instabilities in a brittle crystal. Nature, 455(7217): 1224-1227

Kermode JR, Ben-Bashat L, Atrash F, Cilliers JJ, Sherman D, and De Vita A (2013) Macroscopic scattering of cracks initiated at single impurity atoms. Nat. Commun. 4, 2441-8

Knauss WG (1966) Stresses in an Infinite Strip Containing a Semi-Infinite Crack. J. Appl. Mech. 33(2), 356-362

Lawn BR (1993) Fracture of brittle solids. Cambridge University Press, Cambridge.

Love AEH (1920) A treatise on the mathematical theory of elasticity. Cambridge University Press, Cambridge

Mal AK, Singh SJ (1991) Deformation of Elastic Solids. Prentice Hall, New Jersey

Maranganti R and Sharma P (2007), Phys. Rev. Lett. 98, 195504.

Marder MP and Liu X (1993), Phys. Rev. Lett. 71, 2417.

Marder MP (2004) Effects of atoms on brittle fracture. Int. J. Fract. 130(2):517-555

Moras G, Choudhury R, Kermode JR, Csányi G, Payne MC, and De Vita A (2010), in Trends Comput. Nanomechanics Transcending Length Time Scales, Springer, Berlin

Nair AK, Warner DH, Hennig RG, and Curtin WA (2010), Scr. Mater. 63, 1212.

Rhee YW, Kim HW, Deng Y and Lawn BR (2001) Brittle Fracture versus Quasi Plasticity in Ceramics: A Simple Predictive Index. J. Am. Ceram. Soc., 84(3): 561-565

Rivlin RS, Thomas AG (1953) Rupture of rubber. I. Characteristicenergy for tearing. J. Polym. Sci., 10(3):291-318

Slepyan, L. I. (2002). Models and Phenomena in Fracture Mechanics. Berlin: Springer.

Stillinger FH and Weber TA (1985) Computer simulation of local order in condensed phases of silicon. Phys. Rev. B, 31(8):5262

Swadener JG, Baskes MI, Nastasi M (2002) Molecular Dynamics Simulation of Brittle Fracture in Silicon. Phys. Rev. Lett., 89(8):85503-4

Tadmor EB, Phillips R, Ortiz M (1996) Mixed atomistic and continuum models of deformation in solids. Langmuir, 12:4529-4534

Thomson R, Hsieh C, Rana V (1971) Lattice Trapping of Fracture Cracks. J. Appl. Phys. 42(8), 3154-3160

Wong FS, Shield RT (1969) Large plane deformations of thin elastic sheets of neo-hookean material. Zeitschrift f*ür* Angewandte Mathematik und Physik (ZAMP), 20(2):176199

Xi XK, Zhao DQ, Pan MX, Wang WH, Wu Y, Lewandowski JJ (2005) Fracture of Brittle Metallic Glasses: Brittleness or Plasticity. Phys. Rev. Lett. 94(12):125510-13

Zimmerman JA, Webb EB, Hoyt JJ, Jones RE, Klein PA, and Bammann DJ (2004) Calculation of stress in atomistic simulation. Model. Simul. Mater. Sci. Eng. 12, S319-S332